**CGU HS Committee on River Ice Processes and the Environment**
15th Workshop on River Ice
*St. John's, Newfoundland and Labrador, June 15 - 17, 2009*

# Investigation of the use of GPR for characterizing river ice types

**Francis Bérubé[1], Normand Bergeron[1], Yves Gauthier[1] and Yves Choquette[2]**
*1. Institut national de la recherche scientifique - Centre Eau, Terre et Environnement*
*490 rue de la Couronne, Québec (Québec), G1K 9A9, Canada.*
*2. Institut de Recherche d'Hydro-Québec (IREQ)*
*1800 Blvd Lionel Boulet, Varenne (Québec), Canada, J3X 1S1*
*Francis.Berube@ete.inrs.ca, Normand.Bergeron@ete.inrs.ca,*
*Yves.Gauthier@ete.inrs.ca, choquette.yves@ireq.ca*

Ground penetrating radar (GPR) is now frequently used in river ice studies to provide rapid and continuous measurements of river ice thickness and river bed topography. However, very few studies have investigated the potential utilization of GPR to characterize river ice types, despite the importance this variable exerts on the soundness of the ice cover. In this paper, we analyze GPR measurements from various ice cover types and develop a model capable of measuring the relative proportion of different types of ice in the ice column. Having different electromagnetic properties, the different types of ice are discriminated according to their absorption coefficient of electromagnetic waves. Using the relative intensities of the multiple echoes produced by ice-water interfaces, the model determines the proportion of clear ice in relation to total ice thickness. Validation of this approach on the St-Charles and Batiscan Rivers (Québec, Canada) show strong and significant relationships between the observed and predicted percentage of clear ice ($p<0.001$, $r^2$ of .98 and 0.85 respectively).

## 1. Introduction

Being able to determine the physical characteristics of a river ice cover is important for public safety and navigation, as well as for the prediction and mitigation of ice jams. Depending on the hydro-climatic conditions occurring at freeze-up, various types of ice can form, each possessing very different mechanical properties (Iliescu, 2007) that require specific management strategies. However, despite the important role of river ice type on ice cover soundness, very few attempts have been made to develop means of characterizing river ice types.

Ground Penetrating Radar (GPR) has been used for several years to provide rapid and continuous measurements of river ice thickness (Healy, 2007) The functioning principle of ice thickness measurement from the GPR is based on the delay time of an electromagnetic impulse between the surface and the interfaces formed by the changes in the dielectric properties of the materials (in this case, ice-water interface). Because of their distinct physical characteristics, various forms of ice possess different electromagnetic properties (Table 1), which in turn, affect differently the behaviour of the electromagnetic waves generated by the GPR. In this paper, we develop a modeling approach using variations in the dielectric losses of the electromagnetic waves to characterize the various ice types present in the ice column.

## 2. GPR Background

Starting from Maxwell equations (1), it is possible to calculate the parameters of the theoretical diffusion of the electromagnetic waves generated by the GPR in various materials

$$\Delta e(x, y, z, t) = \sigma\mu \frac{\partial e}{\partial t} + \varepsilon\mu \frac{\partial^2 e}{\partial t^2} \quad [1]$$

where $\sigma, \mu, \varepsilon$ respectively represent conductivity, magnetic permeability and dielectric permeability. The Fourier transform of (1) according to time leads to the wave equation or Helmholtz equation (2)

$$\Delta E(x, y, z, \omega) = -k^2 E(x, y, z, \omega) \quad [2]$$

$$k = \sqrt{\omega^2 \varepsilon\mu + i\omega\sigma\mu} \quad [3]$$

where *k* represents the complex wavenumber. A solution of Helmholtz equation in 1D (z) can be written

$$E(z, \omega) = E(0, \omega) \exp(ikz) = E(0, \omega) \exp(-\alpha z) \exp(i\beta z) \quad [4]$$

Equation 4 represents a vertically propagated wave (z) with a phase speed $\omega / \beta$ and a controlled attenuation by the absorption coefficient $\alpha$. Taking the square of Equation 3 and equalizing the

real part with the imaginary part and then, after algebraic manipulations, the attenuation coefficient (5) is obtained,

$$\alpha = \omega \sqrt{\frac{\varepsilon_e^{'} \mu}{2} \left[ \sqrt{1 + \left( \frac{\varepsilon_e^{''}}{\varepsilon_e^{'}} \right)^2} - 1 \right]} \qquad [5]$$

or simply (6)

$$\alpha = \frac{\sigma \sqrt{\mu}}{2\sqrt{\varepsilon}} \qquad [6]$$

Thus, the enfeeblement of the electromagnetic wave will be dependent on the dielectric constant of the environment as well as on the frequency of the GPR. During the use of a GPR on ice covers, the electromagnetic energy reflected by the ice-water interface is related to the dielectric contrast of the materials given by the Fresnel equation (7).

$$R = \frac{\sqrt{\varepsilon_1} - \sqrt{\varepsilon_2}}{\sqrt{\varepsilon_1} + \sqrt{\varepsilon_2}} \qquad [7]$$

The echo energy resulting from the ice-water interface measured by the GPR will thus be connected to the electromagnetic enfeeblement coefficient of the ice as well as to the reflection coefficient of the ice-water interface. The various types of river ice have slightly different dielectric constants. The electromagnetic energy measurements performed by the GPR can be used in a mathematical model characterizing dielectric constants of the ice and thus, ice types present. If the signal is sampled at a constant phase, equation (4) can be simplified to retain solely the real part of (4)

$$E_z = E_0 \exp\{-\alpha z\} \qquad [8]$$

By applying a natural log on each side of equation 7

$$\ln(E_z) = \ln(E_0) - \alpha z \qquad [9]$$

The slope of the variation of the electromagnetic field along z is controlled by $\alpha$. The difference between two energy peaks of multiple reflections in the ice layer is proportional to the absorption coefficient (equation 10).

$$\alpha \propto \Delta E \qquad [10]$$

From equation 6, the relation between the dielectric permeability and $\Delta E$ is obtained (11).

$$\varepsilon \propto \frac{1}{\Delta E} \propto \text{ Type of ice} \qquad [11]$$

## 3. Method and site sampling

Data for the experiment were obtained in February 2009 on two southern Québec rivers (Canada): the St-Charles River near Québec City (46º48'N) and the Batiscan River, near Trois-Rivières (46º31'N). These two rivers are tributaries of the Saint Lawrence River. The ice cover of the St-Charles River test site was snowfree and had a thickness of 3 to 30 cm. The Batiscan River test site had ice thicknesses of 30 to 60 cm and a snow cover which varied from 0 to 70 cm. At randomly chosen locations on the ice cover of the test sites, GPR measurements were acquired with a SIR-3000 model from the GSSI Company (900 MHz antenna) and ice cores were extracted. For each core, the various ice types were visually identified and measured by an experienced technician. Three types of ice were identified from the ice cores: snow ice, frazil ice and clear ice (columnar ice) (Figure 1).

## 4. Results

The starting hypothesis was that the intensity of the echo measured by the GPR could predict the type of ice present. During sampling, the GPR was configured in automatic gain to avoid signal saturation (Figure 2a). In postprocessing, gain removal was applied to standardize the intensities of the measured signals (Figure 2b). Typically, the ice column was composed of three distinct layers. At the center, a layer of frazil ice that was formed by the dynamic accumulation of drifting frazil ice floes and pans. At the bottom, a layer of clear ice having grown thermally after the consolidation of the frazil ice layer. Sometimes, at the top, a layer of snow ice. GPR signals typically showed the presence of multiple reflections (Figure 2b, 1, 2 and 3). The intensity of echoes 1 and 2 were used as variables for the mathematical model of ice types prediction. The reflection coefficient (equation 7) is assumed to be constant between ice sampling. These values have a scale in Bins for a maximal value of 64000. Dielectric constants of frazil ice and snow ice being very similar, these two types of ice were merged as being a single type. Thus the model attempted to predict the proportion of clear ice with regard to the total thickness of the ice column. From equation (11), a non-linear model is developed (12):

$$P = \frac{C_1}{C_2 E_1 - C_3 E_2} \qquad [12]$$

where P is the percentage of clear ice, $C_i$ are constants and $E_i$ are the energies measured in the echo 1 and 2 by the GPR. The model is numerically resolved by the Levenberg-Marquardt least squares method (13)

$$S(x) = \sum_{i=1}^{m} \left[ y_i - f\left(t_i | a\right) \right]^2 \qquad [13]$$

By applying this model to the St-Charles River data set, relation [14] was obtained (Figure 3).

$$P = \frac{27.8}{-0.00928E_1 + 0.0149E_2} \quad [14]$$

The same process was applied to the Batiscan River data set for which relation 15 was obtained (Figure 4).

$$P = \frac{3802836}{-2E_1 - 9E_2} + 11 \quad [15]$$

Thus, the validation of this approach on the St-Charles and Batiscan Rivers show strong and significant relationships between the observed and predicted percentage of clear ice ($p<0.001$, $r^2$ of .98 and 0.85 respectively).

It is suggested that the somewhat weaker prediction quality for the Batiscan river ($R^2 = 0.85$) could be related to the presence of a snow cover at that site. Indeed, residuals of the model are not correlated to the thickness of ice ($R^2 = 0.017$) nor to the percentage of clear ice ($R^2 = 0.15$). It is believed that the variable density of the snow cover could explain the present variations in the Batiscan river data. Variation of the model parameters between the two rivers could also be explained by the presence of a snow cover on the Batiscan. Furthermore, variations of the electrical conductivity of the two rivers could explain some of the offset between the models.

## 5. Conclusion

In this paper, we analyze GPR measurements from various ice cover types and develop a model capable of measuring the relative proportion of different types of ice in the ice column. Having different electromagnetic properties, the different types of ice are discriminated according to their absorption coefficient of electromagnetic waves. Using the attenuation of the electromagnetic wave generated by the GPR as the criteria, a mathematical model predicting the proportion of clear ice was successfully developed.

Future improvement of the model should focus on integrating the absorption coefficient of the snow cover in order to isolate more precisely the properties of ice cover.

## 6. Acknowledgements

Financial support was provided by the Institut de Recherche d'Hydro-Québec (IREQ).

## 7. References

Bano, M., 2004. Modelling of GPR waves for lossy media obeying a complex power law of frequency for dielectric permittivity. Geophysical Prospecting, 52, p. 11-26.

Cooper, D.W., Mueller, R.A. and Schertler, R.J. 1976. Remote Profiling of Lake Ice using an S-band Short-Pulse Radar aboard an All-Terrain Vehicule. Radio Science, 11, p. 375-381.

Evans, S., 1965. The Dielectric Properties of Ice and Snow. A Review, Journal of Glaciology. 5 p. 773-792.

Healy, D., Katapodis, C. and Tarrant, P., 2007, Application of Ground Penetrating Radar for River Ice Surveys. 14th Workshop on the Hydraulics of Ice Covered Rivers.

Iliescu, D., Baker, I., 2007, The structure and mechanical properties of river and lake ice. Cold Regions Science and Technology. 48, p. 202-217

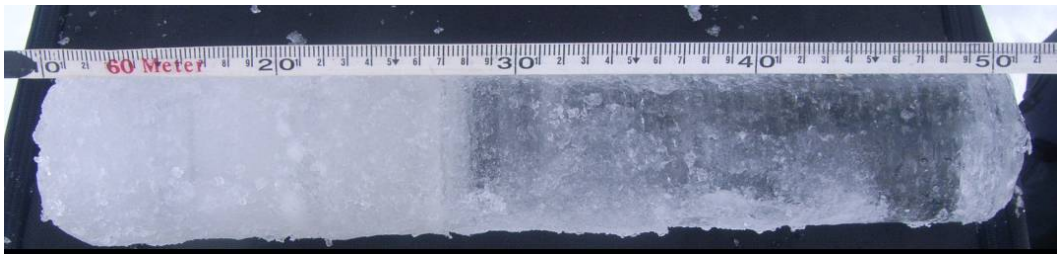


Figure 1. Example of an ice core from the Batiscan River.

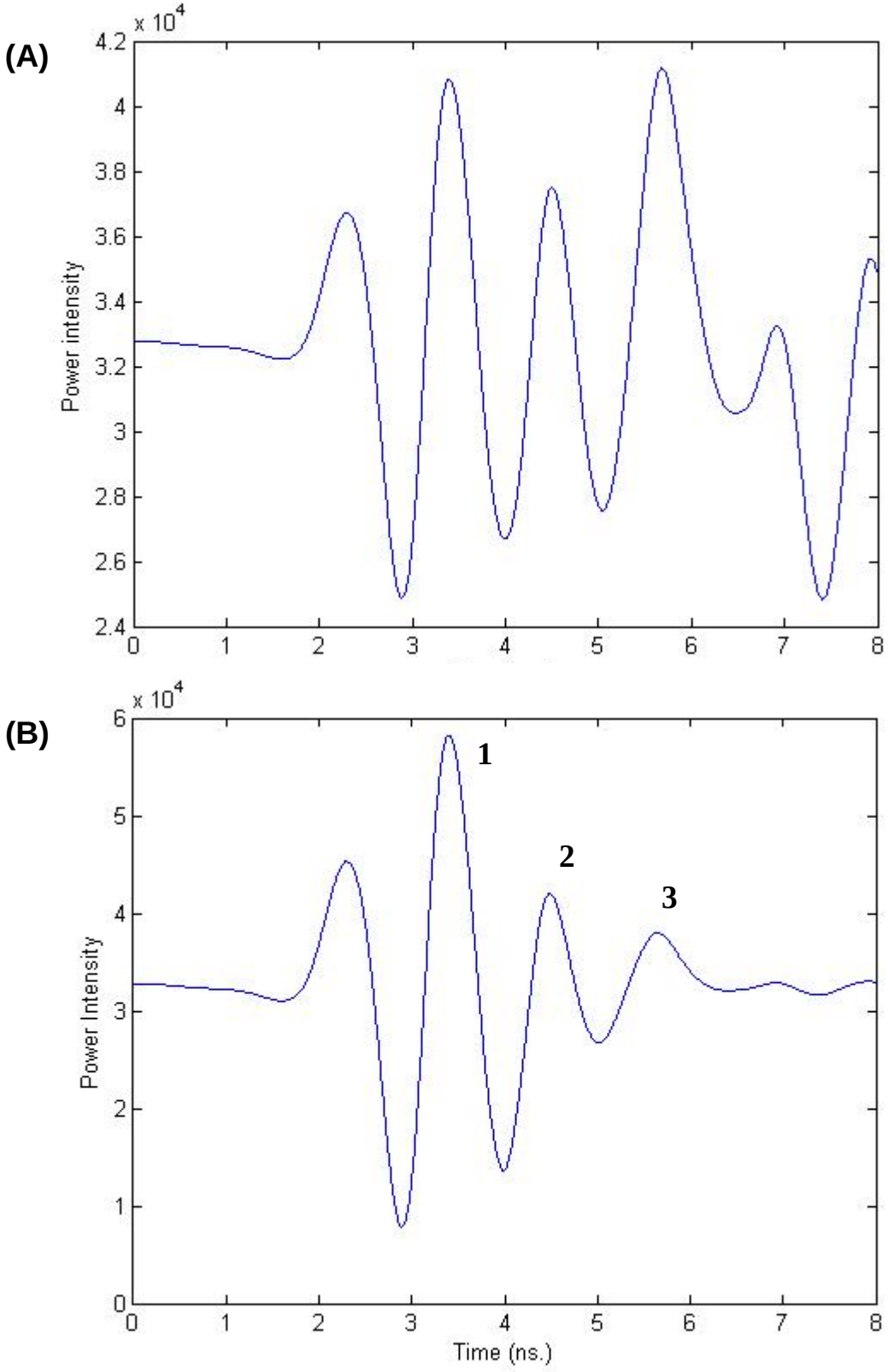


Figure 2. Example of a GPR signal before (A) and after (B) applying the gain remover procedure.

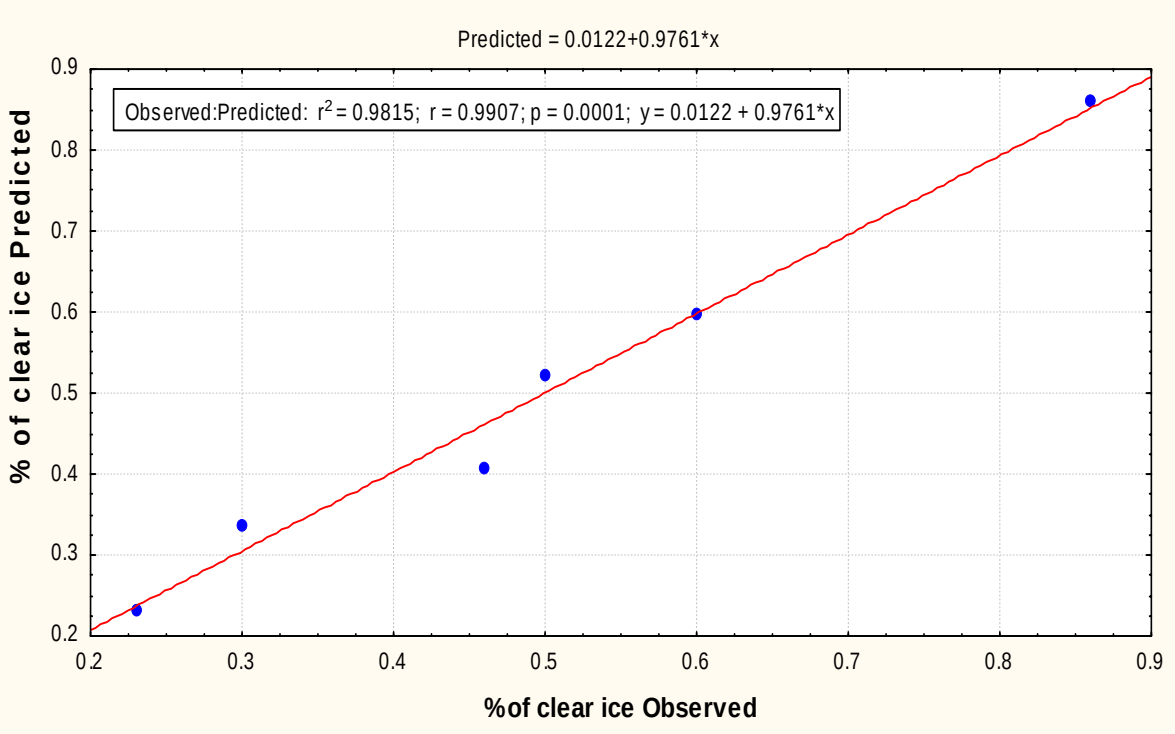


Figure 3. Prediction St-Charles River, absence of snow over the ice layer.

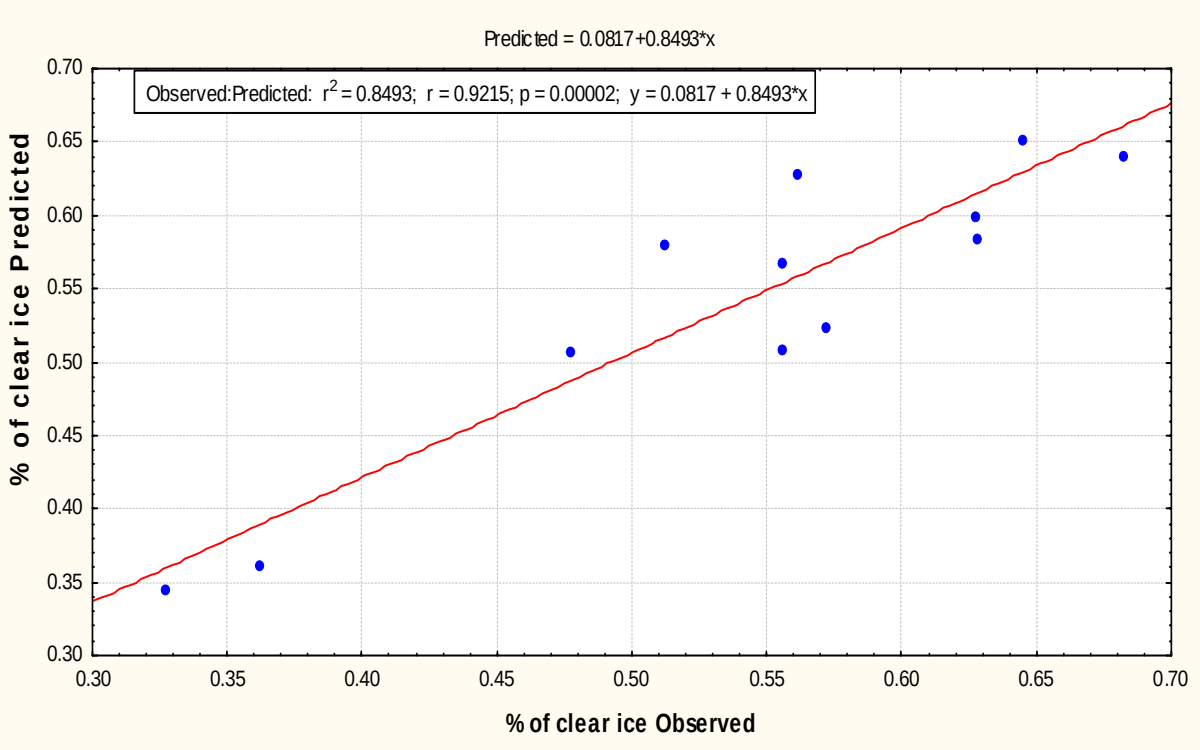


Figure 4. Prediction Batiscan River, presence of snow over the ice layer.

Table 1. Dielectric constant values for different ice types.

| | Dielectric constant | Source |
|---|---|---|
| Clear ice with air bubbles | 2.99 | Cooper et al. (1976) |
| Milky ice | 3.08 | Cooper et al. (1976) |
| Clear ice | 3.17 | Evans (1965) |